UPTEC X 22010
Examensarbete 30 hp
Juni 2022

UPPSALA UNIVERSITET

Intracellular Membrane Remodeling Mechanisms Revealed by Cryo-EM

Sigrid Mack

Civilingenjörsprogrammet i molekylär bioteknik

UPPSALA UNIVERSITET

Intracellular Membrane Remodeling Mechanisms Revealed by Cryo-EM

Sigrid Mack

Abstract

Endophilin B1 (EnB1) is a BAR protein located in the cytosol that controls membrane dynamics of different organelles such as the mitochondria and the Golgi, as well as autophagosomes. It has been suggested that this protein coordinates membrane remodeling events during essential cell death processes. For instance, previous studies show that knockdown of EnB1 leads to dysregulation of mitochondrial dynamics and inhibition of apoptosis. This protein could thereby have a critical tumor suppressor role in the cell. Despite the important role of EnB1 in many intracellular signaling processes, some parts of its underlying mechanisms of function are still unknown, more specifically, what drives the protein to bind to the membrane and what the protein structure looks like when bound.

Since EnB1 plays an important role in many intracellular trafficking events, it is of interest to obtain more information about this protein, both about its structure and membrane binding interactions. New information on this subject will contribute to a better understanding of how EnB1 modulates intracellular membranes to control several critical trafficking processes that contribute to neuron degradation and carcinogenesis.

This specific project aims at designing membrane templates that support EnB1 membrane-binding and bending for evaluation of binding capacity and for structural characterization by cryo-EM, and other associated methods.

To study the binding interactions of EnB1, different protein constructs were first expressed and purified. Membrane templates (liposomes and nanodiscs) were then created to enable structural characterization as well as studying the binding capacity of EnB1 to different lipids. A lipid binding assay with multiple variants of liposomes were created to study the biding capacity of EnB1, and negative stain transmission electron microscopy, as well as cryo-electron microscopy was used for visualization of the templates. By analyzing the data from the lipid binding assay, it can be concluded that both lipid composition and membrane curvature affects EnB1 membrane binding. The cryo-EM visualization also confirm that EnB1 is involved in membrane remodeling.

Teknisk-naturvetenskapliga fakulteten

Uppsala universitet, Utgivningsort Uppsala/Visby

Handledare: Anna Sundborger-Lunna Ämnesgranskare: Sebastian Barg

Examinator: Peter Kasson

Populärvetenskaplig text:
Cancer är en sjukdom som drabbar en stor del av befolkningen. Under sin livstid kommer en av tre i Sverige att bli diagnostiserad med denna sjukdom. Trots omfattande forskning finns det fortfarande många okända mekanismer i cellen som kan spela en stor roll för utvecklingen av cancer. En sådan typ av betydande mekanism är den reglerande membranbindningen av proteinet Endophilin B1(EnB1).

Tidigare studier visar att frånvaro av EnB1 i cellen kan leda till en onaturlig reglering av mitokondriens dynamik. Detta kan i sin tur leda till att programmerad celldöd hämmas. Dessa resultat indikerar att EnB1 har förmågan att koordinera förändringar i membranet under naturliga celldödsprocesser, och verkar därför ha en kritisk roll för att dämpa tumörutveckling i cellen. I koppling till detta har EnB1 påvisats vara frånvarande vid flertalet cancersjukdomar; prostatacancer, tarmcancer, magsäckscancer samt cancer i gallblåsa och urinblåsa.

Trots den kritiska roll som EnB1 verkar ha i många av cellens signaleringsprocesser, är dess underliggande funktionsmekanismer till en stor del okända. Det är därför av relevans att ta reda på mer kring hur EnB1 ser ut strukturellt och hur det binder till olika membran för att få en bättre och mer detaljerad förståelse för hur detta protein fungerar för att kontrollera ett flertal kritiska processer som bidrar till neurodegenerativa sjukdomar och utvecklingen av cancer.

I detta projekt har olika typer av membranmodeller designats för att efterlikna det naturliga yttre mitokondriemembranet för att främja inbindningen av EnB1. Den ena membranmodellen som gjordes var *nanodiscar*, med avsikten att använda dessa tillsammans med kryo-elektronmikroskopi för att ta reda på hur EnB1 ser ut strukturellt vid inbindningen. Denna typ av elektronmikroskop har möjligheten att återskapa en mycket detaljerad tredimensionell avbild av en biomolekyl. *Liposomer* är en annan typ av membranmodell som gjordes med syftet att studera vilka typer av komponenter i ett cellmembran som EnB1 binder bäst till.

Experimenten med liposomerna visade bland annat att specifika kombinationer av olika typer av membrankomponenter påverkar inbindningen av EnB1. Resultaten visar även att EnB1 generellt sett föredrar att binda till membran med en lägre kurvatur. Utformningen av den andra membranmodellen, nanodiscarna optimerades även under projektets gång för att erhålla funktionella komplex för optimal strukturell karakterisering.

Resultaten från detta projekt kan användas som utgångspunkt för att utforma riktade experiment med syftet att i detalj ta reda på mer kring vad som orsakar den reglerade membranbindningen av EnB1. De optimerade nanodiscarna kan även användas för att skapa en detaljerad strukturell avbild att proteinet vid membranet. Dessa vidarestudier har potential att vara värdefulla i bland annat cancerforskningssyfte.

List of abbreviations

CL	Cardiolipin
Cryo-EM	Cryogenic electron microscopy
DLS	Dynamic light scattering
EnA1	Endophilin A1
EnB1	Endophilin B1
IMAC	Immobilized metal affinity chromatography
LUV	Large unilamellar vesicles
MOM	Mitochondrial outer membrane
MSP2N2	Membrane scaffolding protein 2
SEC	Size exclusion chronotherapy
SEM	Standard error of the mean
SUV	Small unilamellar vesicles
TEM	Transmission electron microscopy

1 Introduction

1.1 Endophilin B1

Membrane remodeling is a common and critical event in many cellular processes. One protein family involved in many of these critical events is the Bin/Amphiphysin/Rvs167 (BAR) protein family. BAR domains are highly conserved dimerization domains found in proteins involved in the membrane dynamics of the cell (Simunovic *et al.* 2015). Dimeric BAR domain proteins are normally shaped like crescents with a concave side that facilitates the binding to curved membranes. The BAR domain is in other words able to sense membrane curvature. Most BAR proteins contain varying lipid specificity domains, which facilitate the targeting process of the protein to specific compartments of the membrane (Salzer *et al.* 2017).

The BAR family consists of three subgroups: N-BAR, F-BAR, and I-BAR proteins. One N-BAR protein of importance in a variety of intracellular trafficking events is *Endophilin B1* (EnB1). EnB1 is a peripheral membrane protein with two amphipathic helices: H0 at the N-terminal BAR domain, H1i, as well as an SH3 domain at the C-terminal. H0 has proven to be essential for membrane binding of N-BAR proteins and H1i or *helix1 insert*, has shown to be important for curvature generation and scaffolding of N-BAR proteins. (Salzer *et al.* 2017). When H0 binds to the membrane, H1i is also hypothesized to follow along and insert into the membrane. The insertion of the H1i, along with the crescent shape of the N-BAR domain, is believed to be the factors contributing to the curvature generation and scaffolding (Bhatt *et al.* 2021) (Masuda *et al.* 2006).

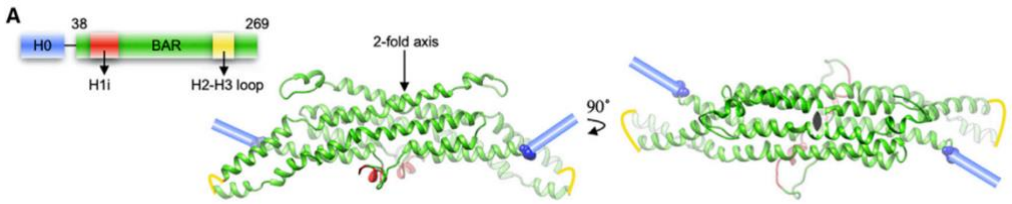

Figure 1. Homology model of EnB1 N-BAR dimer (80 kDa). The amphipathic helix H0 in blue and H1i in red. From *Amphipathic Motifs Regulate N-BAR Protein EnB1 Auto-inhibition and Drive Membrane Remodeling*, by Bhatt et al, 2021.

An important function of this N-BAR protein is to promote autoinhibition that is suggested to be mediated by the mechanism of H0-SH3 domain interactions (Bhatt *et al.* 2021). The EnB1 membrane remodeling process is thus controlled by autoinhibition, which is mediated by interactions between the H0-SH3 domains. EnB1 has also proven to assemble into helical scaffolds on membranes as well as being able to drive membrane binding and formation by interactions between the H0 helix and the lipid bilayer of the membrane. By taking these aspects into account, as well as the fact that amphipathic motifs are capable of membrane binding by sensing packing defects, it has been hypothesized that a specific combination of phospholipids and packing defects contributes to H0-SH3 dissociation, which enables membrane binding of the H0 helix.

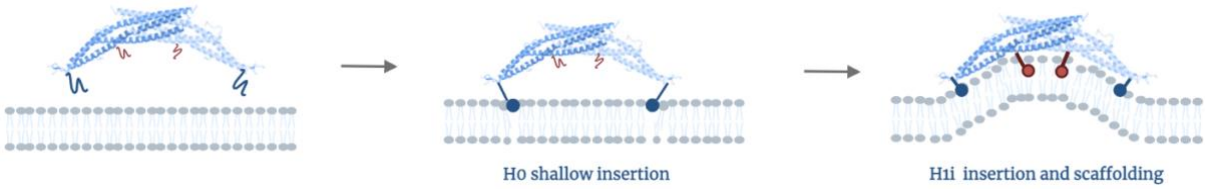

Figure 2. The hypothesized process of EnB1 membrane binding. The H0 helices (in dark blue) bind to a specific membrane site. The crescent shape of the EnB1-dimer in combination with the H1i insertion (in red) into the membrane is then hypothesized to be responsible for curvature generation and scaffolding.

Downregulation of EnB1 causes several critical intracellular trafficking events to take place and influences the regulation of cell fate decisions, such as mitochondrial fission. These morphological changes could for instance lead to abnormal regulation of mitochondrial dynamics and inhibition of apoptosis (Bhatt *et al.* 2021). This suggests that EnB1 is involved in critical cell death processes and could thereby have an important tumor-suppressing role in the cell.

1.2 Membrane proteins & techniques for analysis

As mentioned in the beginning, EnB1 is a peripheral membrane protein. This means that EnB1 interacts with the lipid bilayer of membranes and is able to attract both integral membrane proteins as well as the phosphate heads of the membrane lipids (Lacapère *et al.* 2007). This enables peripheral proteins to interact with the cell membrane, without being anchored. Both peripheral and integral membrane proteins are not easy to study. This is mainly due to the relatively rapid and spontaneous movements of both phospholipids and membrane proteins called *lateral diffusion* (Ramadurai *et al.* 2009). This is an important process utilized by the cells which allow for an intricate structural and dynamic reorganization of proteins. Consequently, membrane proteins cannot be statistically localized to a specific area of the cell membrane.

To overcome these difficulties, several structural-based methods have been utilized in recent years. Techniques such as electron microscopy enable the study of membrane proteins with atomic resolution (Goldie *et al.* 2014). The advancements made by using these microscopy techniques allows for structures with better resolution from less material, at a faster rate, and from a broad spectrum of membrane protein targets.

Negative stain transmission electron microscopy (TEM) is a technique that is commonly used to visualize purified membrane proteins and to assess the quality of the sample (De Carlo & Harris 2011). A heavy metal stain is first added to a grid with the protein sample to increase the contrast. The stained sample can then be analyzed with TEM, by being subjected to a beam of electrons. An image of the sample is then obtained based on how the electrons passes through the sample on the grid. Negative stain TEM is a simple and straight forward technique to study the homogeneity of a sample. However, the process is done in a non-native environment.

Another prominent electron microscopy method used for studying biomolecules at near atomic resolution, is single-particle cryo-electron microscopy (cryo-EM) (Doerr 2016). With this method, the native structure of the protein can be persevered by rapid freezing prior to analyzation with TEM. As explained above, a stream of electrons is directed towards the sample. The electrons pass though the sample and are then captured by a camera that creates

images based on how the electrons passes through. Multiple images called 2D classes is then collected from each sample. Since a low electron dose is used to minimize the risk of damaging the sample, the resulting 2D images often have background noise that doesn't allow for studying the sample in atomic detail. This can be solved by averaging a multitude of induvial particles. Image processing software is then used to recombine the 2D images to create a 3D reconstruction of the sample.

Another advantage of using cryo-EM, except for obtaining high resolution information, is that this technique can be used to study organelles, different macromolecular complexes as well as proteins with a high molecular weight (Lyumkis 2019). A disadvantage with this technique is the low signal to noise ratio which can results in low contrast images. Cryo-EM is also a costly method.

X-ray crystallography is an alternative method that can be used for structural characterization (Zheng *et al.* 2015). This method also provides high-resolution information and is relatively cheap and simple to use. However, one major drawback with this method is the fact that the protein must be crystallized which in some cases are impossible and can in other cases cause irreversible changes to the structure.

The methods used in this project to study EnB1 bound to different membranes are negative stain TEM and cryo-EM.

1.3 Mitochondrial outer membrane

As previously mentioned, downregulation of EnB1 can lead to abnormal regulation of mitochondrial dynamics caused by morphological changes (Karbowski *et al.* 2004). The mitochondria are intracellular organelles found in almost all human cells. They are essential for aerobic metabolism and energy production through oxidative phosphorylation. They are also involved in metabolic pathways including beta-oxidation, the Krebs cycle, and the synthesis of iron-sulfur clusters, and in the import and assembly of proteins (Kühlbrandt 2015). The mitochondria also play an important role in apoptosis, the production of reactive oxygen species (ROS), calcium homeostasis, and the maintenance of lipid membrane. This is thus an organelle that is essential for a normal cell to function properly.

The mitochondria have four main compartments; the intermembrane space with a similar composition to the cytosol, the inner membrane where the respiratory chain proteins, the matrix where most of the metabolic reactions take place and the mitochondrial outer membrane (MOM) surrounds the whole organelle and forms a barrier and is selectively permeable to certain ions and small molecules (Kühlbrandt 2015).

EnB1 has been shown to bind to the MOM under normal conditions in the cell (Karbowski *et al.* 2004). The absence of EnB1 causes morphological changes, leading to atypical regulation of mitochondrial dynamics and finally apoptosis.

1.4 Membrane templates

To be able to study Endophilin and its binding mechanisms in more detail, mimics of the mitochondrial outer membrane can be used to enable binding and tubulation. Membrane mimics are useful tools for investigate the interplay between proteins an lipids, as well as for structural studies of proteins and functional studies of lipids (Sarkis & Vié 2020). Negative stain TEM, cryo-EM and binding assays can then be used to study the complexes in further detail.

1.4.1 Liposomes

Liposomes are artificial vesicles made of lipids. These vesicles can vary in size, from small unilamellar vesicles (SUVs) with a diameter of 20-100 nm to large unilamellar vesicles (LUVs) with a diameter of 100-1000 nm (Emami *et al.* 2016). Liposomes can be created to resemble a native environment to membrane proteins, and are therefore useful tools for studying lipid-protein binding and tubulation of membrane proteins. The unilamellar vesicles in this project are created by extruding a lipid mix through a filter of a specific size. When the protein of interest is added to the liposomes, the binding ability can be determined by an SDS-PAGE and the tubulation studied with negative stain TEM.

The lipid composition, as well as the size of the liposomes, can be varied to study how the protein of interest interacts in under different conditions.

EnB1 has shown favor binding to certain membrane lipids such as cardiolipin (Etxebarria *et al.* 2009) and is also hypothesized to cluster this lipid amongst others, when binding to the mitochondrial outer membrane. Liposomes based of different lipid compositions and sizes have therefore been created in this project to study how EnB1 interacts with different types of membrane mimics.

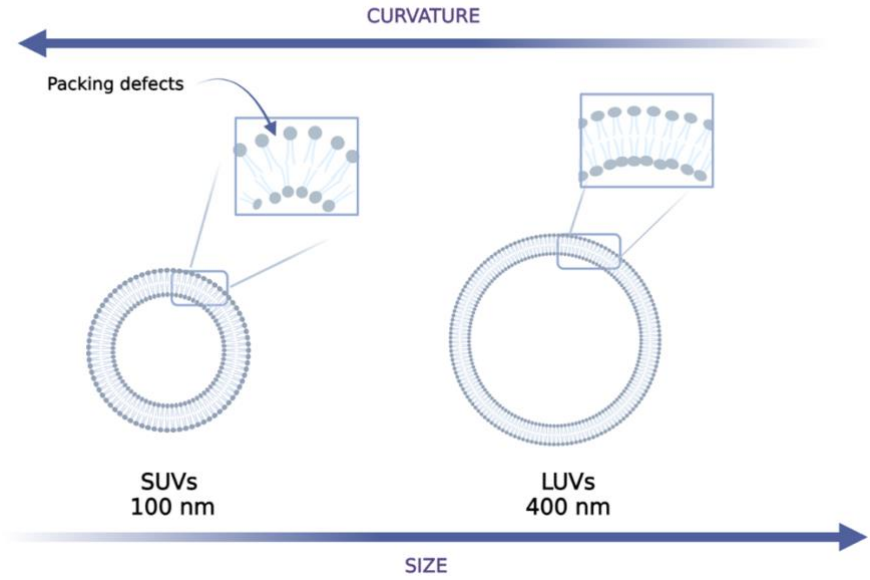

Figure 3. Comparison between liposomes with high and low curvature. SUVs have a higher membrane curvature and thereby more packing defects. LUVs have a lower curvature and less packing defects.

To study how the membrane curvature affects EnB1 binding, SUVs with a diameter of 100 nm and LUVs with a diameter of 400 nm were created for each lipid mix.

The main questions to be answered with the different liposomes created in this project are:

- *How does lipid composition affect endophilin membrane binding?*
- *How does membrane curvature affect endophilin membrane binding?*

EnB1 has shown to selectively bind to cardiolipin (CL) enriched membranes (Etxebarria *et al.* 2009). This suggests that EnB1 may cluster CL as well as other non-lamellar membrane forming phospholipids in the mitochondrial membrane. The process of clustering is hypothesized to function by the EnB1 favored binding to certain lipids on the membrane surface, which will attract more of these specific lipids to the binding site. This will in turn attract more EnB1 to the membrane surface. If EnB1 were to cluster CL, and other lipids in the outer membrane of the mitochondria, it could result in membrane remodeling which in turn could lead to membrane permeabilization and cell death. It is therefore of interest to create membrane mimics with different lipids to study the binding capacity of EnB1.

Cardiolipin has an important role in the cell by regulating several mitochondrial proteins (Dudek 2017). Examples of these are phosphate kinases, electron transport complexes, and different carrier proteins. Cardiolipin contains four acyl chains and has the ability to form non-lamellar structures. These structures are considered to be important for both membrane structure and function. This lipid has also shown to be cone-shaped and causes thereby positive membrane curvature (see Figure 4). Cardiolipin is a mitochondria-specific phospholipid, which means that this lipid is exclusively found in this organelle (Falabella *et al.* 2021)..

Cholesterol has also been hypothesized to important for EnB1 membrane binding. This organic sterol molecule has an amphiphilic nature, and its structure contains a hydroxyl group that is able to form hydrogen bonds with phospholipids (Paila & Chattopadhyay 2010). This sterol has shown to play an important role in membrane organization, such as regulation of membrane permeability, strength, elasticity, and stiffness. Cholesterol is often used in the making of liposomes since it can contribute to enhanced membrane stability as well as prevent aggregation (Nakhaei *et al.* 2021). This sterol has shown to be shaped like an inverted cone and causes thereby negative curvature (see Figure 4).

Phosphatidylinositol 4,5-bisphosphate or PIP_2 belongs to the phosphoinositide family and is a negatively charged lipid that plays an important role as a membrane-bound molecule with the ability to anchor proteins (Balla 2013). It has also been shown to have a local impact on the lipid bilayer that surrounds it. This disorder in the lipid bilayer is caused by an orientation difference of the PIP_2 headgroup relative to the other lipids. This perturbation causes a specific distance-dependent assembly of the lipids (their heads are oriented closer to the bilayer normal) that surrounds PIP_2 (Borges-Araújo & Fernandes 2020). PIP_2 can also be described as a cone-shaped lipid and causes thereby positive membrane curvature (see Figure 4). This lipid is of interest to study since it plays an important role in Endophilin A1 (a protein similar to EnB1) membrane binding (Chang-Ileto *et al.* 2011). Endophilin A1 has shown to cluster PIP_2 in the MOM (Shukla *et al.* 2019). This is because its positively charged helix (H0) is drawn to the negatively charged PIP_2 regions on the membrane (Chang-Ileto *et al.* 2011). EnB1 has on the other hand another sequence in the helix which in theory makes it less inclined for membrane binding under these conditions (Bhatt *et al.* 2021). It can therefore be speculated that EnB1 isn't recruited to the membrane with PIP_2. To find out if PIP_2 is important for EnB1 binding and recruitment, and to determine if this speculation mentioned above is correct or not, another question that can be asked from this:

- *Is PIP_2 important for the recruitment of EnB1 to the membrane?*

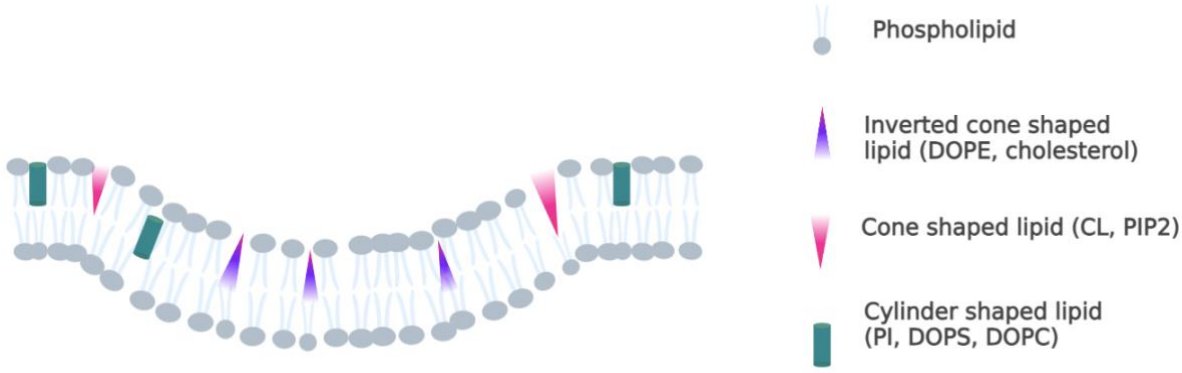

Figure 4. Negative curvature caused by the lipids shaped like inverted cones. Cylinder shaped lipids does not cause any membrane curvature. Cone-shaped lipids contributes to positive curvatures while lipids shaped like inverted cones contribute to negative curvature.

Several other lipids have been used in this project to make different lipid mixes such as PI, DOPS, DOPE, and DOPC. The mentioned lipids have different structures; DOPE and cholesterol are shaped like inverted cones, while PI, DOPS, and DOPC are cylindrical shaped and cardiolipin and PIP_2 are shaped like inverted cones (Zhukovsky *et al.* 2019). Different combinations of all these lipids create membrane mimics with varying curvatures and thereby varying packing defects. Lipids shaped like cylinders doesn't cause any membrane curvature, while cone-shaped lipids cause positive curvature (Elías-Wolff *et al.* 2019) and lipids shaped like inverted cones cause negative curvature (Wang *et al.* 2007).

1.4.2 Nanodiscs

Nanodiscs are self-assembled synthetic membrane model systems that can be used to reconstitute membrane proteins in an artificial environment resembling the native membrane. The usual diameter of nanodiscs is between 10-20 nm (Bayburt & Sligar 2010). The discs are composed of a membrane scaffolding protein with amphipathic helices and a lipid bilayer of phospholipids with a hydrophobic edge. This nanodisc-protein complex will facilitate the studying of the lipid-protein binding interactions (Denisov & Sligar 2016).

The small diameter of the discs enables EnB1 binding but makes polymerization of the protein impossible (Denisov & Sligar 2016). Nanodiscs can thus be used to study the protein-membrane binding without the membrane being disrupted by tubulation or other events, that can be caused by EnB1 polymerization. These structures can in other words preserve the first step of protein binding to the membrane and can be described as a controlled bilayer surface for the study of membrane proteins.

In this project, nanodiscs with a lipid composition of 100% DOPS are used to study the binding interactions of EnB1. DOPS is phospholipid with a negatively charged headgroup at a physiological pH (Lipa-Castro *et al.* 2021).

1.5 Aim of this project

Despite the crucial role of EnB1 in numerous intracellular signaling events, the underlying membrane-binding mechanism of this protein is not well understood. The aim of this project is to obtain a better understanding of what drives membrane binding by studying the environment in which the amphipathic helix H0 and BAR domain is able to interact with the lipid bilayer of the membrane. This is achieved by designing membrane templates of different

lipid compositions that support EnB1 membrane-binding and bending. By evaluating the binding mechanism to these different types of membranes, more information about which lipid compositions enable membrane binding of EnB1 will be obtained. The outstanding question that will be addressed is: *how does EnB1 interact with mimics of different intracellular membranes?*

New information on this subject will contribute to a better understanding of how EnB1 modulates intracellular membranes to control several critical trafficking processes that contribute to neuron degradation and carcinogenesis.

2 Materials and methods

2.1 Protein expression and purification

Three proteins were expressed and purified during this project: EnB1, SUMO protease, and membrane scaffolding protein 2 (MSP2N2).

The protein of interest, EnB1, was purified with affinity chromatography using gravity columns and size exclusion chromatography (SEC) with a Bio-Rad NGC System. The SUMO protease was purified with affinity chromatography using gravity columns and was later used to cleave off a SUMO tag fused to EnB1. This tag was cleaved to ensure that it wouldn't affect or disrupt the results of the upcoming assays.

MSP2N2 was purified with affinity chromatography using gravity columns. This scaffolding protein is required for the nanodisc structural assembly. See 3.3.2 *Nanodisc assembly* for details of how this purified protein was used.

2.1.1 EnB1

E. coli (BL21strain) was used for the expression of the EnB1 with a pET28 vector carrying a kanamycin resistance gene. The EnB1 construct encodes for a SUMO tag as well as a C-terminus 12xHis-tag. To regulate the expression of this recombinant protein, a T7 promoter can be induced by IPTG. The pET28 vector was modified by Veer Bhatt, a former co-worker of Anna Sundborger-Lunna.

2.1.1.1 Expression

A small amount of glycerol stock was added to 50 mL Luria Broth (LB) with kanamycin added to a final concentration of 50 ug/mL (LB_{kan50}). The flask was incubated with shaking overnight at 37°C. The O/N culture was added at a 1:1000 dilution to baffled 3 L flasks containing LB_{kan50}. The flasks were incubated with shaking at 125 rpm at 37°C until OD_{600} reached a value of 0.5 and was then induced by the addition of 0.2 mM IPTG. The expression was then continued O/N at room temperature (RT).

The following day, the cell suspension (3 L) was pelleted by centrifugation at 7000 rpm for 20 min using a J-Lite™ JLA-9.1000 Fixed-Angle Rotor (Beckman Coulter). The supernatant was discarded, and the pellet was resuspended in 50 mL EnB1 lysis buffer (20 mM Tris, 500 mM NaCl, 20 mM Imidazole, pH 8.2, 0.2 mM DTT, 0.25% Triton-X 100).

2.1.1.2 Purification

The cell suspension was sonicated (Vibra Cell ™, SONICS) with the following settings: amp 70%; time 30: pulse 02/08 seconds. After sonication, the sample was centrifuged at 17 000 rpm for 1 h using an SS-34 Fixed Angle Rotor. Immobilized metal affinity chromatography (IMAC) was used for the first purification step of EnB1. The supernatant from the centrifugation was added to a disposable gravity column with Ni-NTA-resin (ThermoFisher Scientific) and incubated at 4℃ with gentle agitation for 1 h. The flow-through (FT) from the column was discarded and the resin was washed with 6% EnB1 elution buffer (20 mM Tris, 500 mM NaCl, 500 mM Imidazole, pH 8.2, 0.2 mM DTT). The protein was incubated with EnB1 elution buffer for 10 min before elution. The elution process was repeated three times. Vivaspin 20 Centrifugal Concentrators 30 kDa cutoff (Sartorius) were used with a SX4400 swinging bucket rotor at 4000 rpm for 20 min. Size exclusion chromatography (SEC) on the NGC system (Bio-Rad) was finally used for further purification. The Superdex 200 10/300 GL column (Cytiva) was equilibrated with 2 column volumes (CVs) of EnB1 SEC buffer (20 mM HEPES, 150 mM NaCl, 1 mM TCEP, pH 8.1) before loading the sample onto a 500 ul loop with a syringe. The flow rate was set to 0.5 ml/min and the sample was eluted with the same buffer and collected by fractionation. The sample was finally concentrated again with the same spin concentrators as mentioned above.

2.1.2 SUMO protease

E. coli cells were used for the recombinant production of the SUMO protease. The plasmid carries a kanamycin resistance gene and encodes for an N-terminal 6XHis-tag. To regulate the expression of this recombinant protein, a T7 promoter can be induced by IPTG.
The glycerol stock used for the expression of this protease consisted of *E. coli* BL21(DE3) transformed cells prepared by Veer Bhatt.

2.1.2.1 Expression

A small amount of glycerol stock was added to 50 mL Luria Broth (LB) with kanamycin added to a final concentration of 50 ug/mL (LB_{kan50}). The flask was incubated with shaking overnight at 37℃. The O/N culture was added at a 1:1000 dilution to baffled 3 L flasks containing LB_{kan50}. The flasks were incubated with shaking at 125 rpm at 37℃ until OD_{600} reached a value of 0.6 and was then induced by the addition of 0.2 mM IPTG. Three hours post-induction, the cell suspension was pelleted by centrifugation at 7000 rpm for 20 min using a J-Lite™ JLA-9.1000 Fixed-Angle Rotor (Beckman Coulter). The pellet was resuspended in 50 mL Protease lysis buffer (20 mM Tris, 500 mM NaCl, 20 mM Imidazole, 0.25% Triton-X100, pH 8.2, 0.2 mM DTT + 1 protease inhibitor tablet).

2.1.2.2 Purification

The cell suspension was sonicated with the following settings: amp 70%; time 30: pulse 02/08 seconds. After sonication, the sample was centrifuged at 17 000 rpm for 1 h using an SS-34 Fixed Angle Rotor. IMAC was used for the first purification step of His-SUMO protease. The supernatant from the centrifugation was added to a disposable gravity column with Ni-NTA-resin (ThermoFisher Scientific) and incubated at 4℃ with gentle agitation for 1 h. The flow-through (FT) from the column was discarded and the resin was washed with 6% Protease elution buffer (20 mM Tris, 500 mM NaCl, 500 mM Imidazole, pH 8.2, 0.2 mM DTT). The protein in the column was then incubated for 10 min before elution with the Protease elution buffer. The elution process was repeated three times.

2.1.2.3 SUMO tag cleavage

The SUMO tag of EnB1 was cleaved off with the His-SUMO protease. Prior to the cleavage, a buffer exchange was performed for SUMO tagged EnB1 by using a PD-10- column (Cytiva) equilibrated with cleavage buffer (20 mM Tris, 250 mM NaCl, 0.5 mM DTT, pH 8.0). His-SUMO EnB1 was then added to a dialysis tubing (3 kDa cutoff) and put in cleavage buffer at 4℃ for 3 hours. The His-SUMO protease was then added to the tubing and put in fresh cleavage buffer O/N at 4℃. The cleavage EnB1 was then collected from the tubing and purified according to the same instructions as described on page 13.

2.1.3 Membrane scaffolding protein (MSP2N2)

2.1.3.1 Transformation

For the transformation of MSP2N2, 1 ul DNA was added to one 50 ul vial of BL21(DE3) (Invitrogen) competent cells and incubated on ice for 15 min. The vial was then heated shocked at 42℃ for 40 sec and incubated on ice for 2 min. 450 mL s.o.c medium (Invitrogen) was then added to the vial and a 1-hour incubation at 100 rpm in 37℃ was then started. The suspension was finally added to LA plates with a 50 ug/mL resistance with glass beads.

2.1.3.2 Expression and harvest

A small amount of glycerol stock was added to 50 mL Luria Broth (LB) with kanamycin added to a final concentration of 50 ug/mL (LB_{kan50}). The flask was incubated with shaking overnight at 37℃. The O/N culture was added at a 1:1000 dilution to baffled 3 L flasks containing LB_{kan50}. The flasks were incubated with shaking at 125 rpm at 37℃ until OD_{600} reached a value of 0.5 and was then induced by the addition of 0.2 mM IPTG. Three hours post-induction, the cell suspension was pelleted by centrifugation at 7000 rpm using a J-Lite™ JLA-9.1000 Fixed-Angle Rotor (Beckman Coulter). The pellet was resuspended in 50 mL MSP2N2 lysis buffer (20 mM Tris, 500 mM NaCl, 20 mM Imidazole, pH 8.2, 0.2 mM DTT+ 0.25% Triton-X 100).

2.1.3.3 Purification

The cell suspension was sonicated with the following settings: amp 70%; time 30: pulse 02/08 seconds. After sonication, the sample was centrifuged at 17 000 rpm for 1 h using an SS-34 Fixed Angle Rotor. IMAC was used for the first purification step of His-SUMO protease. The supernatant from the centrifugation was added to a disposable gravity column with Ni-NTA-resin (ThermoFisher Scientific) and incubated at 4℃ with gentle agitation for 1 h. The flow-through (FT) from the column was discarded and the resin was washed with 6% MSP2N2 elution buffer (20 mM Tris, 500 mM NaCl, 500 mM Imidazole, pH 8.2, 0.2 mM DTT). The protein in the column was incubated for 10 min with elution buffer before elution. The elution process was repeated three times. To concentrate the sample to 2.4 mL, Vivaspin 20 Centrifugal Concentrators 30 kDa cutoff (Sartorius) using a SX4400 swinging bucket rotor at 4000 rpm for 20 min, was then used to concentrate the sample to 0.5 mL. A PD-10 column (Cytiva) was then used for changing the buffer to a standard nanodisc buffer (20 mM Tris (pH 7.4), 0.1 M NaCl, 0.5 mM EDTA). The sample was finally concentrated once again to 1.5 mL with the same spin concentrators as mentioned above.

2.2 Evaluation of protein expression and purification

To evaluate the protein expression and purification, SDS-PAGE and Western Blot was used. The SDS-PAGE was used for EnB1, SUMO protease and MSP2N2 to study how the protein

content differed during the whole process. This was done by taking samples at different timepoints in the expression and purification processes for all protein constructs and loading them onto a gel. Western Blot was used to validate the purified constructs. In this project, EnB1 and MSPN2N was validated with this method.

SDS PAGE

Any kD Mini-PROTEAN TGX Stain-Free Gel (BIO-RAD) was used with a 6X sample buffer (375 mM Tris.HCl, 9% SDS, 50% Glycerol, 0.03% Bromophenol blue) to load 10 ul sample into each well. The Precision Plus Protein Standards #161-0374 ladder was used. SDS-PAGE running buffer (0.025 M Tris Base, 0.192 M glycine, 1% SDS) was then added to the cassette. The gels were run at 180 V for approximately 40 min. The gels were then stained with InstantBlue® Coomassie Protein Stain (Expedeon) and destained with dH_2O.

Western Blot

To confirm the purification of the proteins of interest, a western blot for MSP2N2 and EnB1 respectively was performed. Firstly, an SDS-PAGE was run with the sample of interest according to the description above. The gels were then put in WB transfer buffer (25 mM Tris, 192 mM glycine, 20% methanol (vol/vol), pH 8.3). for 10 min before membrane transferring with Trans-Blot turbo machine (BIO-RAD) with the Trans-Blot Turbo Transfer Pack (BIO-RAD). The membranes were then washed with WB wash buffer (1X TBS 0.1% tween) and then put in blocking buffer (5% milk in X TBS 0.1% tween) O/N at 4°C. WB wash buffer was added to the membrane again for 1 h before adding primary antibodies with a ratio of 1:500 and incubating on gentle agitation for 1 h. The membrane was washed three times with WB wash buffer for 10 min at 4°C prior to the addition of secondary antibodies with a ratio of 1:10 000. The membrane was then developed using an NBT/BCIP Tablet (Roche).

The primary antibodies used for EnB1 was anti-EnB1 polyclonal Goat antibody (Invitrogen) and alkaline phosphatase conjugated antibodies (Sigma-Aldrich) were used as secondary. For the MSP2N2 western blot, anti-polyHis monoclonal mouse antibody (Sigma-Aldrich) antibodies were used. The secondary antibodies used were also alkaline phosphatase conjugated antibodies (Sigma-Aldrich)

2.3 Creation of MOM mimics

2.3.1 Lipid preparation

The lipid films used for the nanodiscs, and the liposomes were prepared by adding a total of 50 ul lipids dissolved in chloroform (10 mg/ml concentration) to a glass vial. The lipids were then dried using a stream of N_2 and put in a desiccator in room temperature (RT) until used.

2.3.2 Nanodisc assembly

The lipid film was dissolved in 225 ul ND standard buffer (20 mM Tris (pH 7.4), 0.1 M NaCl, 0.5 mM EDTA) and 0.5% DDM and put in a 37°C ultrasonication water bath for 1 h. By dissolving the lipid film in 250 ul buffer and DDM, a final lipid concentration of 2 mg/ml was obtaine. The DDM detergent was added to solubilize the lipids. For the nanodiscs in this project, 100% 18:1 DOPS was used. The assembly mixture with a ratio of 1:10 (MSP2N2:

DOPS) was made by adding the scaffolding protein, the lipid mix, and ND standard buffer to a total volume of 500 ul. The molar ratio was calculated using the concentration of MSP2N2 (1.43 mg/ml) and DOPS (2 mg/ml). The mix was then incubated at RT for 45 min. The self-assembly of the discs was then started by removing the DDM with dialysis. The incubated mix was added to dialysis tubing with a 3.500 MW cut-off and put in ND standard buffer. The buffer was changed three times during 24 hours. The sample was then loaded onto a Superdex 200 10/300 GL column (Cytiva) with a 500 ul loop coupled to an ÄKTA system (Cytiva) with a flow rate of 0.5 ml/min. Fractions corresponding to the expected size of the nanodiscs were then collected and frozen in liquid nitrogen (LN_2) and stored at 80°C.

To bind EnB1 to the discs, the protein was added to the discs with a ratio of 1:2.5 (nanodiscs: EnB1). The sample was then incubated for 1h at RT prior to evaluation and characterization.

2.3.3 Nanodisc validation

Dynamic light scattering (DLS)

To validate the assembly of the nanodiscs, Dynamic Light Scattering (DLS) was used to study the diameter of the discs. The cuvette was first washed five times with MQ water. 20 ul sample was then added to the cuvette before placing it in the DLS W130i system (Avid Nano). The setting used with the pUNk software was then used with the following settings: Intensity: 668 135 counts/s; Temperature: 20°C; Laser 100%; Attenuator 100%; MW model: Globular Proteins.

Negative stain transmission electron microscopy (TEM)

Negative stain TEM was also used to get visual confirmation of the nanodisc assembly. The sample of interest was added to glow-discharged carbon-coated mesh grids and left on for 30 seconds before removal with paper. The grids were then negatively stained using 2% uranyl acetate and analyzed with a FEI Tecnai G2 F20 microscope.

Native gel

To study if EnB1 was successfully bound to the discs, native gels were performed. Native gel electrophoresis is run under native conditions and separates the sample components based on charge and hydrodynamic size. Native gel running buffer (10X; 25 mM Tris, 192 nM glycine, pH 8.3) was added to the cassette. The samples were loaded onto any kD Mini-PROTEAN TGX Stain-Free Gel (BIO-RAD) with 1X Native gel samples buffer (62.5 mM Tris, 40% glycerol, 0.01% bromophenol blue) and run at 30 V for 5 h in 4°C.

2.3.4 Liposome binding assay

The lipid films from the desiccator were dissolved in 250 ul Liposome Buffer (20 mM HEPES, 150 mM NaCl, 1 mM TCEP, pH 8.1) and put on a shaker for 10 min at RT. To create the liposomes, extrusion was performed with 1000 ul syringes (Avanti Polar Lipids). The 100 nm and 400 nm Whatman® Nuclepore™ Track-Etched membranes (Cytiva) were soaked in liposome buffer before extruding 15-17 times to create the liposomes. For the lipid binding assay, 10% liposome mix was added to ultracentrifugation tubes along with Liposome buffer and EnB1 with a final concentration of 0.2 mg/ml. The sample was incubated for 15 min prior to ultracentrifugation for 10 min at 31 900 rpm at 23°C using an S110AT-2244 rotor. To analyze the binding capacity of EnB1 to the liposomes, a sample from the supernatant was taken and the rest was discarded. The pellet with the protein-bound liposomes was then

resuspended in a Liposome Buffer with the same volume as used for the centrifugation. A sample from that suspension was then loaded onto a gel (following the SDS-PAGE protocol) along with the supernatant sample to compare the band intensities and thereby determine the percentage of bound protein.

2.3.5 Statistical analysis

To analyze the band intensities on the gels, ImageJ was used. A picture of the scanned gel was first uploaded, and a 32-bit image type was then selected to change the colors to black and white. After that, each band was selected using a rectangular marker of the exact same size for each band. The lanes were then plotted, and the straight marker was used to select the intensity peak for each band. The area under the curve for each sample was then calculated automatically by integrating the area under each intensity curve using the selected tracing tool.

To visualize the results, the percentage of protein in the supernatant and pellet was calculated and presented as bar graphs using Excel. Standard error bars for each displayed sample set were added to each displayed sample in the bar graph.

The Analysis of variance (ANOVA) test as well as a Post Hoc analysis was also performed to compare different samples. The ANOVA test was first done to test the equality of at least three group means. And to identify the differences between two sample sets, a Post Hoc analysis was done based on the ANOVA analysis.

Both the ANOVA test and Post Hoc analysis were performed using RStudio. See Appendix 7.2 for the script.

2.4 Cryo-EM

Quantifoil™ R 1.2/1.3 mesh grids were first glow-discharged for 1 min. For automated vitrification, a Vitrobot System (ThermoFisher Scientific) was used. Deionized water was used for vapor, and the humidity was set to 95% and the temperature to 4°C. 3 ul of sample was loaded onto each grid and blotted for 3 sec. The grids were then stored in LN_2. For visualization, Glacios™ Cryo-EM 200 kV was used.

3 Results

3.1 EnB1 protein expression & purification

Three protein constructs were expressed and purified in this project. The protein of interest, EnB1 was purified with affinity chromatography and SEC. The final sample was then validated with western blot using EnB1-specific antibodies. Figure 5 below shows the SEC chromatogram for the purification of EnB1 along with the developed membrane for the western blot.

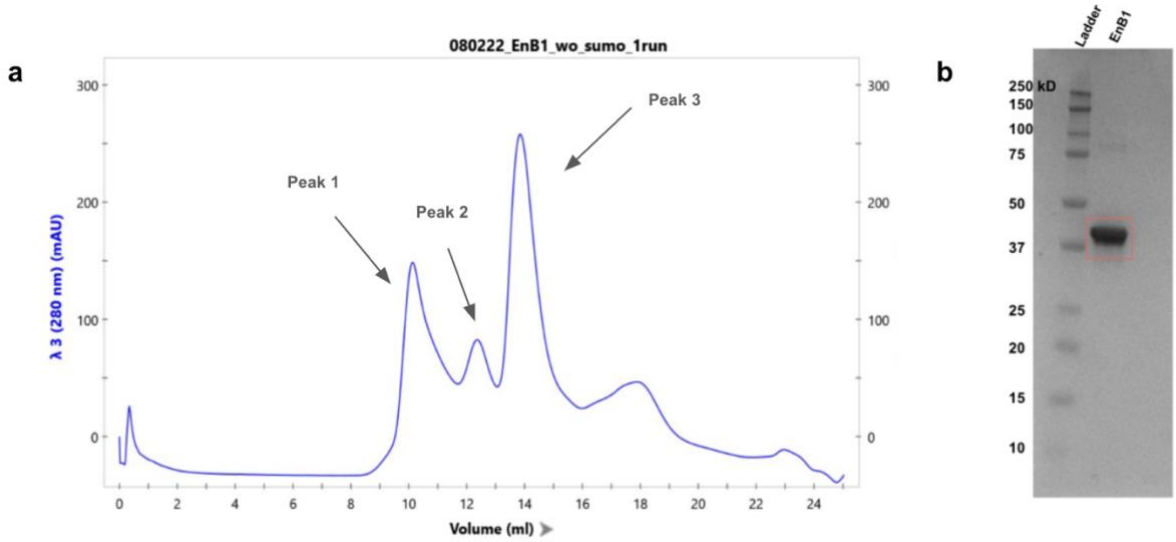

Figure 5. Purification and validation of EnB1 **a** SEC chromatogram for the first purification of EnB1. The y-axis shows the absorbance at a 280 nm wavelength and the x-axis displays the volume in mL **b** result of a western blot using EnB1 specific antibodies to confirm the presence of EnB1 in the sample. The red square marks the resulting band at 42 kDa, corresponding to the molecular weight of EnB1.

This SEC chromogram displays three significant peaks. The fractions from 13 -14.5 mL corresponding to peak 3 (see Figure 5 a) were collected and pooled obtain the protein of interest. Peak 3 corresponds to approximately 84 kDa which is the molecular weight (MW) of a EnB1 dimer.

A western blot with EnB1-specific antibodies was used to validate the collected protein (see Figure 5 b). The distinct band at 42 kDa (corresponds to the MW of a EnB1 dimer) clearly confirms that the protein of interest was successfully expressed, purified, and collected.

3.1.1 Cleavage of the SUMO tag

Since EnB1 was fused with a SUMO tag, a SUMO protease was expressed and purified to cleave off this tag. The reason for this cleavage is to prevent the tag from affecting or disrupting the binding mechanisms of the protein in upcoming experiments/assays. The lanes in the gel below (see Figure 6) represents each step of the cleavage experiment.

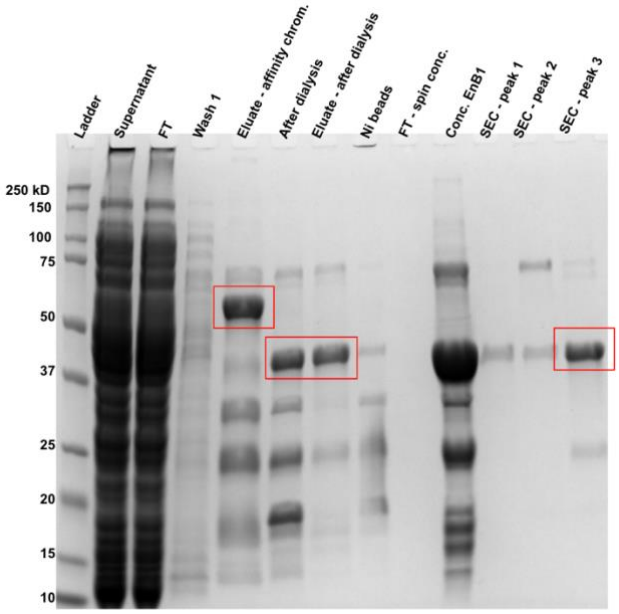

Figure 6. SDS-PAGE result from samples taken in each step of the process to cleave off the SUMO tag from EnB1. The first lane is the ladder, followed by a sample from the supernatant after the centrifugation to pellet the cell debris of the expressed SUMO protease. The third lane *FT* is the flow through of the column after adding the supernatant sample to the gravity column. This is followed by a sample from the first wash, *Wash 1* and the final eluate after the whole affinity chromatography. *After dialysis* is a sample taken after the SUMO protease was used to cleave off the tag from EnB1 followed by an affinity purification again. Sample concentration was then performed (*conc. EnB1*) followed by SEC where three peaks were collected. Most of the EnB1 could be found in the third peak, *SEC – peak 3* as marked with a red square in the figure.

This gel demonstrates the cleavage of the SUMO-his tag with the SUMO protease. Lane 5, Eluate - *affinity chromatography* shows the uncleaved SUMO-EnB1 after affinity purification. In the lane after, *after dialysis*, it can be observed that the tag has been cleaved off. The cleaved EnB1 with a molecular weight of 42 kDa can be observed, as well as the SUMO tag with a molecular weight of approximately 17 kDa can be seen below.
When the fused SUMO tag had been cleaved off with the protease, the final EnB1 protein sample was obtained and could after that be used for experiments with membrane models.

3.2 Nanodiscs

The first membrane template created in this project was nanodiscs (NDs). Several parameters were continuously optimized during the course of the project to enable the optimal conditions for nanodisc assembly. The parameters that were changed or adjusted were the detergent, the ratio of protein to lipids and the method for detergent removal. Figure 7 below displays the general workflow for the nanodisc assembly.

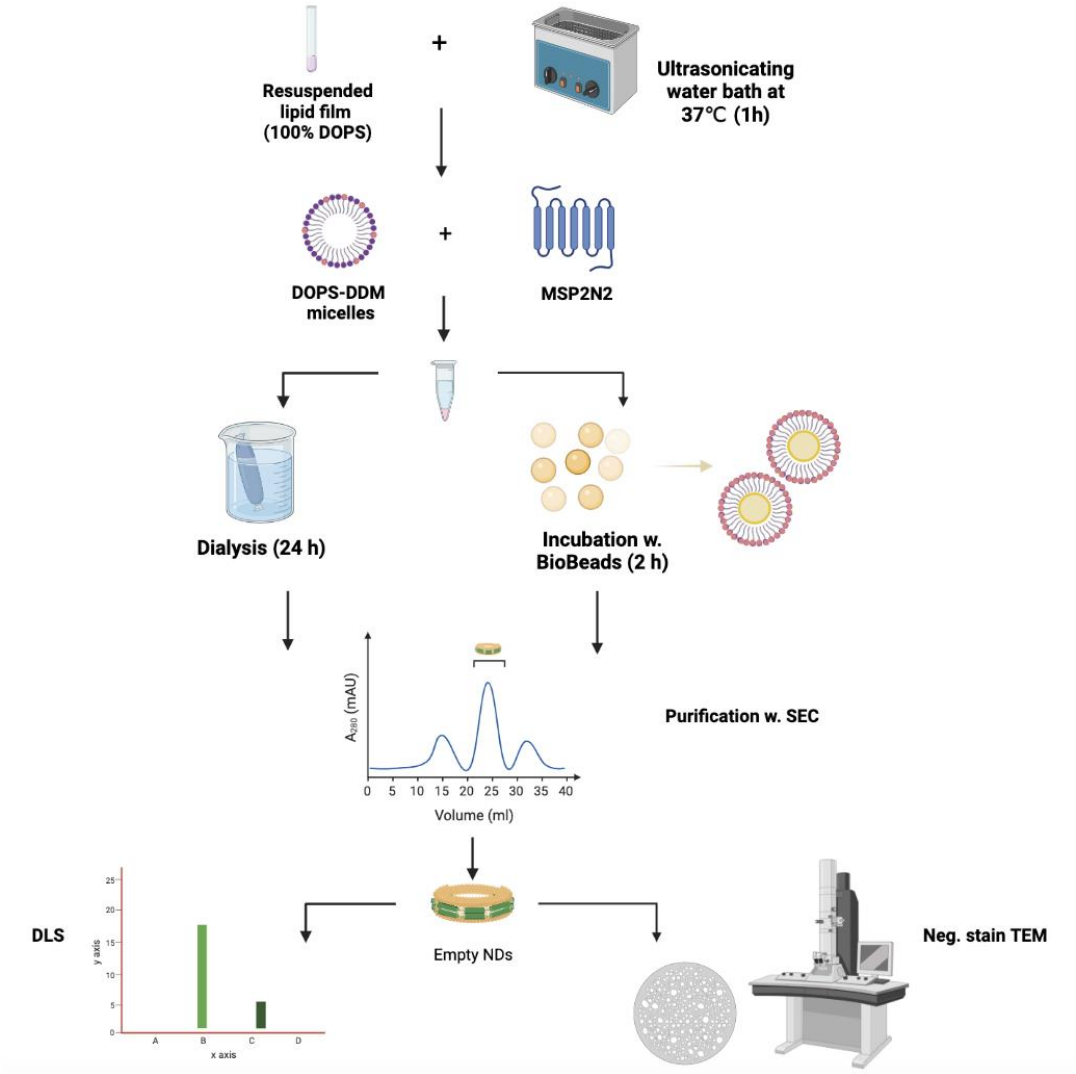

Figure 7. Flowchart of the general workflow of the nanodisc assembly protocol. The resuspended film is first added to an ultrasonic bath before the addition of MSP2N2 and detergent. Both dialysis and BioBeads were tried to remove the detergent. After the removal of detergent and the self-assembly of the discs, SEC was used to obtain a purified sample of empty NDs. DLS and TEM was then used to validate the discs. conform the presence of discs.

Choice of detergent

To solubilize the lipids, a detergent is essential. In this project, both Dodecylmaltoside (DDM) and sodium cholate were tried to ensure optimal solubilization of the lipids before the addition of MSP2N2 for the assembly of nanodiscs. Although the final assembly showed no significant differences between these two detergents, the purification curves looked slightly better with DDM after the detergent removal. See chromatogram in Figure 8 a, where DDM was used.

Protein lipid ratio

Different ratios of protein to lipids were tried during the optimization phase of the project. An excessive amount of lipids would lead to liposome formation, and too much protein would lead to aggregate formation. Both protein aggregation and liposome formation would lead to a non-homogenous sample that would be more challenging to purify and analyze in later steps. The optimal ratio was finally determined to 1:10 (MSP2N2: DOPS).

Removal of detergent

In order to enable nanodisc self-assembly, the detergent is removed. In this project, two different methods of detergent removal were tried to optimize the assembly. Most of the articles recommend using Bio Beads for easy removal. The whole process with the beads is easy to perform and can take as little as 2 hours in total. The other method tried for detergent removal was a 24 h dialysis at RT. Both the BioBeads and dialysis were used multiple times prior to the purification of the discs to obtain a proper assessment of each method. Even though time-consuming, dialysis proved to be the best method for removing the detergent without compromising the rest of the sample. The hydrophobic beads were on the other hand found to be inefficient since the beads appeared to adsorb both the DDM and the lipids. This resulted in non-existing nanodisc self-assembly since the scaffolding protein was left without any lipids for the assembly

3.2.1 Nanodisc purification & MSP2N2 validation

After the detergent removal, the empty discs were purified with SEC. A western blot with His-tagged antibodies was also used to verify the presence of MSP2N2 in the discs.

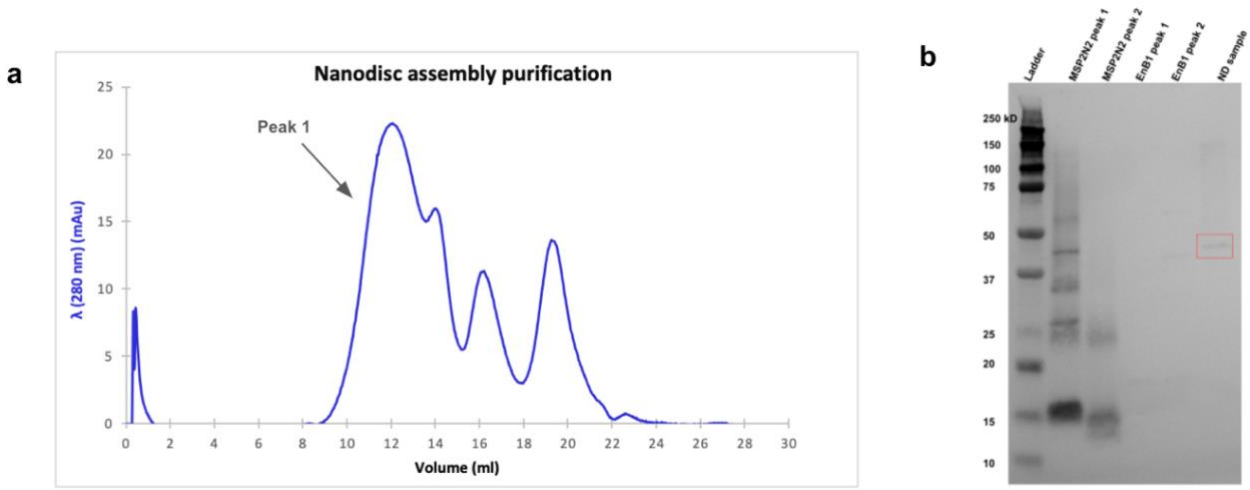

Figure 8. Nanodisc purification and validation of MSP2N2 **a** SEC chromatogram for the purification of the nanodisc assembly. The y-axis shows the absorbance at a 280 nm wavelength and the x-axis displays the volume in mL **b** result of a western blot using His-tagged antibodies to validate the presence of MSP2N2 in the discs. The red square marks the resulting band at 45 kDa, corresponding to the MW of EnB1.

To obtain the purified empty discs, the fractions corresponding to peak 1 were collected (10-14 mL). The MW corresponding to Peak 1 is approximately 90 kDa, which is the hypothesized MW of the protein in an empty nanodisc. It can be observed that the protein concentration in the sample was quite low, by studying the absorbance values on the x-axis (see Figure 8 a). This was later confirmed by measuring the concentration with a Nanodrop™. The final nanodisc sample containing the pooled fractions was therefore concentrated after the SEC.

To confirm that the nanodiscs contained MSP2N2, a western blot with a His tagged antibody was used, since this scaffolding protein is histidine tagged and no MSP2N2 specific antibody was available. The blot confirms the presence of MSP2N2 in the nanodisc sample, but the faint band indicates a low protein concentration (see Figure 8 b).

Optimized nanodiscs

When the optimal assembly conditions were established (see Table 1 below), the discs in the final sample were proceeded to be validated.

Table 1. Summary of the optimal conditions for nanodisc assembly established in this project.

Optimal assembly conditions	
Ratio	**1:10 (MSP2N2: lipids)**
Detergent	**5 % DMM**
Detergent removal	**Dialysis in RT (24h)**
Purification method	**Size exclusion chromatography w. fraction collection**

3.2.2 Nanodisc Validation

To validate the assembly of the discs, negative stain transmission electron microscopy (TEM) and dynamic light scattering (DLS) was used.

3.2.2.1 Negative stain Transmission electron microscopy (TEM)

Negative stain TEM was used to get a visual confirmation of what the sample of assembled nanodiscs.

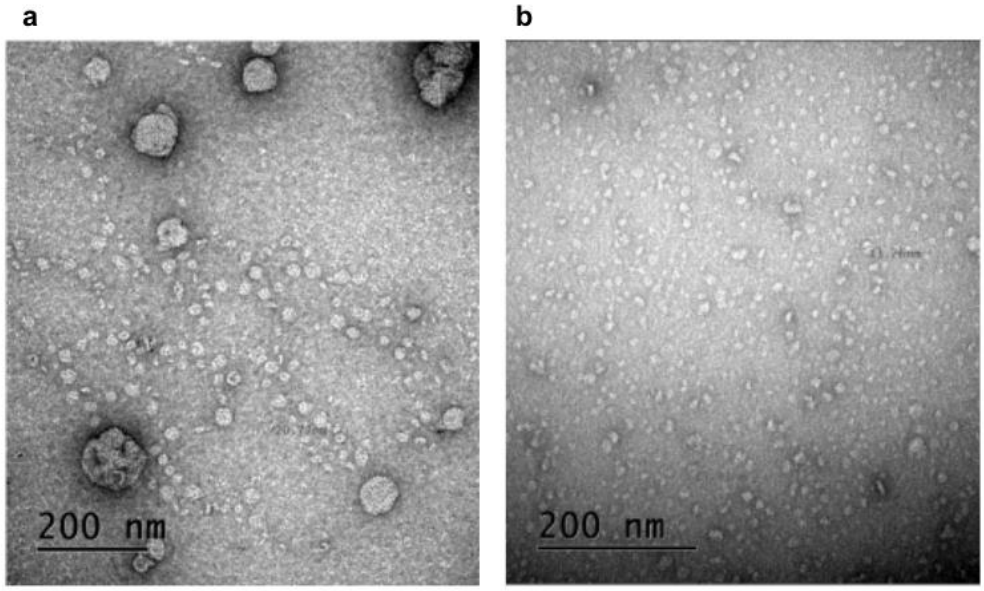

Figure 9. TEM images of nanodiscs **a** nanodisc sample for the first assembly attempt shows an inhomogeneous sample containing only a few nanodiscs **b** nanodisc sample from the latest assembly attempt according to the optimized protocol. The sample appears homogenous with a high density of formed nanodiscs.

The membrane scaffolding protein (MSP2N2) used is expected to create discs with an average diameter of approximately 15 nm. The size of the created discs can be confirmed to be of that approximate diameter by studying the TEM images above.

By comparing Figure 9 a and b, a difference between the sample contents can be observed. The number of discs is higher in the sample where the optimized protocol was used, compared to the sample of the first nanodisc assembly experiment where no optimization had been done. There are also less liposomes present in the optimized sample, compared to the first sample. This improvement was a consequence of an optimized protein to lipid ratio.

3.2.2.2 Dynamic light scattering (DLS)

In addition to the TEM images, DLS was used to measure the diameter of the discs and to obtain a more detailed overview of what the sample contained.

a

Peak #	Mean Dh (nm)	Mode Dh (nm)	Std. Dev. (nm)	Polydisp. (%)	Est. MW. (kDa)	Intensity (%)	Mass (%)	Volume (%)	Number (%)
1	17,21	16,62	2,21	12,82	535,76	2,43	98,53	99,51	100,00
2	88,22	105,61	13,33	15,10	Out of Range	2,56	1,04	0,41	0,00
3	502,22	493,14	249,37	49,65	Out of Range	49,58	0,43	0,08	0,00
4	4 418,21	4 726,91	1 246,35	28,21	Out of Range	33,40	0,00	0,00	0,00
5	609 548,50	591 077,60	160 380,50	26,31	Out of Range	12,03	0,00	0,00	0,00

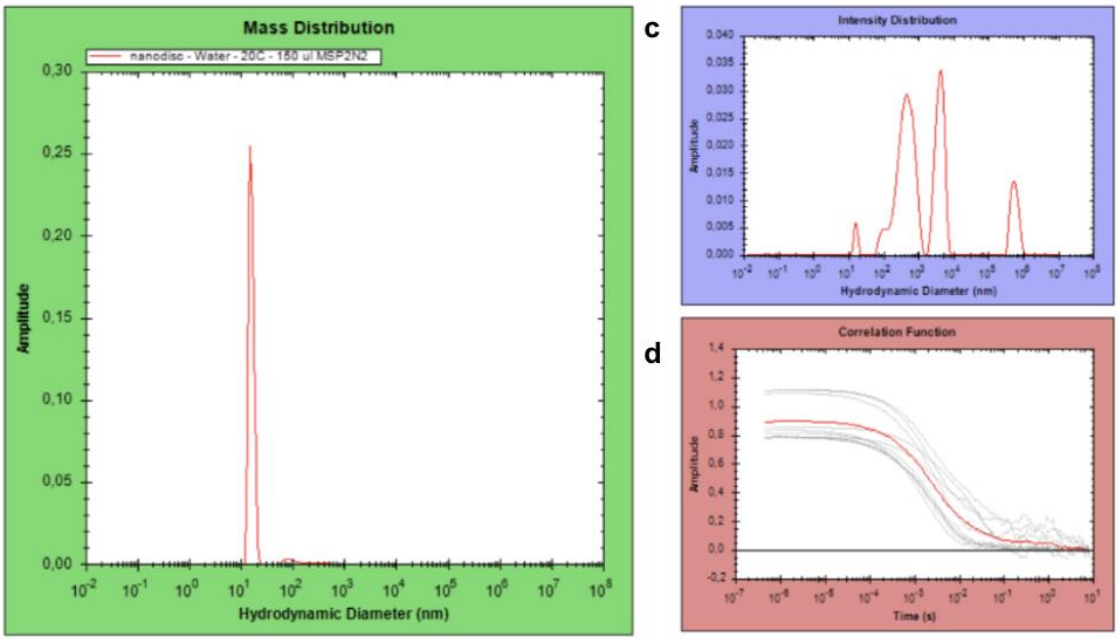

Figure 10. DLS result from the optimized ND sample. **a** table displaying the specific measurements for each type of detected particle in the sample. **b** graph displaying the mass distribution of the sample, showing a significant peak at around 15 nm. **c** graph displaying the intensity distribution of the sample showing the detected masses **d** graph displaying the correlation function of the sample.

As Figure 10 shows, 98.53% of the sample contains particles with a mean diameter of 17 nm and a mode diameter of 16 nm, which corresponds to the expected size of the discs. This can also be seen from the graph displaying the mass distribution of the hydrodynamic diameter particle size. Peak 2-4 with larger masses (see Figure 10 c displaying the intensity distribution) are hypothesized to be liposomes, while peak 5 with a significantly large diameter is believed to be caused by an air bubble in the cuvette. The other 1.47% of the sample (see peak 2 & 3 in Figure 10 a) are most probably liposomes.

3.3 Liposome binding assay

Another part of the project was to create liposomes as membrane models. These models were in this project used to study the binding capacity of EnB1 to liposomes with a varying lipid composition and curvature.

Table 2: Composition of each lipid mix (Mix 1-8). Displayed in molar percentage (%).

Lipid mix	DOPS (%)	DOPE (%)	DOPC (%)	PI (%)	PIP_2 (%)	Cardiolipin (%)	Cholesterol (%)
Mix 1	50	40	-	-	-	5	5
Mix 2	55	40	-	-	-		5
Mix 3	55	40	-	-	-	5	-
Mix 4	-	44	37	9	10	-	-
Mix 5	-	38	33	9	20	-	-
Mix 6	-	50	50	-	-	-	-
Mix 7	-	38	33	9	-	20	-
Mix 8	-	38	46	9	-	7	-

Displayed in Figure 11 below is an overview of the results for all lipid mixes that were created in this project.

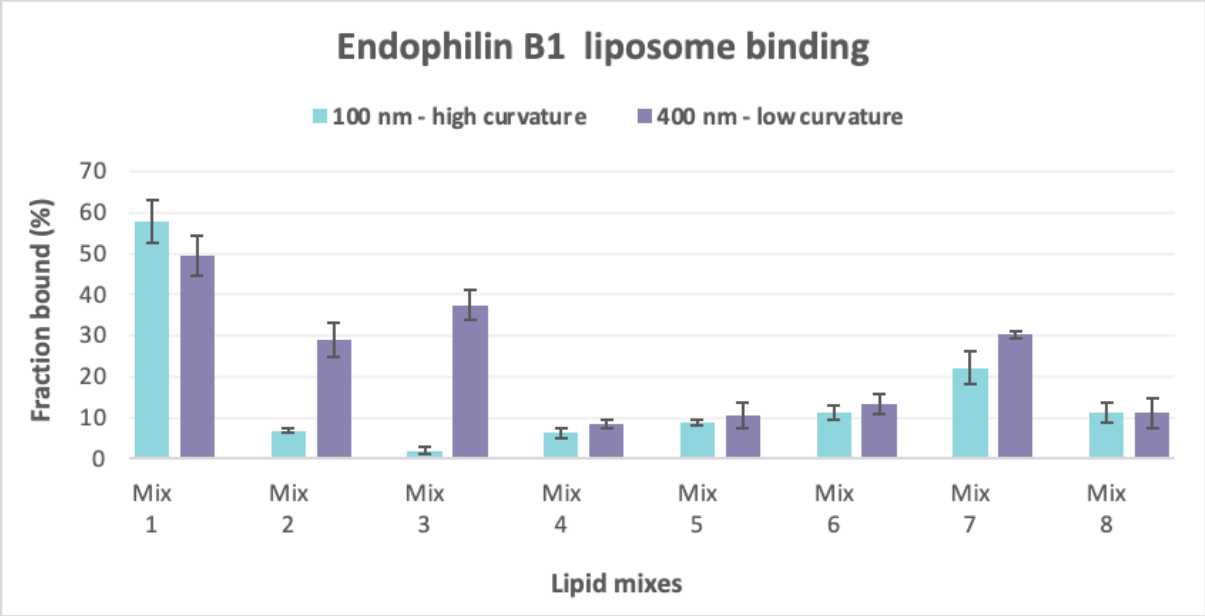

Figure 11. Bar graph displaying the fraction of bound EnB1 to the liposomes created of each lipid mix. Liposomes of a 100 nm and 400 nm size were created for each lipid mix. The y-axis displays the percentage of bound EnB1, and the x-axis display the different liposome mixes. The data used to generate these bars represents the mean ± SEM for each sample set.

This figure displays how the fractions of bound EnB1 differs between every mix and liposome size. See Appendix 7.1 for a complete description of the contents of each mix. To compare different mixes, a statistical analysis with the ANOVA test and Post Hoc analysis was performed to determine if the different comparisons between the samples were statistically significant or not.

Table 3. Three groups were compared with the ANOVA test and Post Hoc analysis. If $p < 0.05$, the result between each comparison is statically significant.

Comparison	P adjusted value	Statistically significant (p <0.05)
Mix 1–Mix 2	0.0004238	Yes
Mix 1–Mix 3	0.0014450	Yes
Mix 2-Mix 3	0.2925326	No
Mix 4-Mix 5	0.0688177	No
Mix 5-Mix 6	0.9230857	No
Mix 4-Mix 6	0.1119182	No
Mix 3-Mix 7	0.2338438	No
Mix 3–Mix 8	0.0131242	Yes
Mix 7-Mix 8	0.0022038	Yes

As Table 3 displays above, Mix 1, 2 and 3 were analyzed to compare the effect of a differing CL and cholesterol content. Mix 1- Mix 2 and Mix 1 - Mix 3 showed statically significant results. This means that there is a statistical difference between these mixes.

When Mix 4, 5 and 6 were analyzed to compare the effect of PI and PIP_2, no statistically significant results were obtained.

Finally, mix 3, 7, 8 were analyzed to study all mixes with CL and no cholesterol. There were no significant results between Mix 3 and 7. Mix 7 compared with 8, as well as Mix 3 and 8 showed however statically significant results.

3.3.1 Different lipids affect the membrane binding of EnB1

One of the main questions to be answered with this lipid binding assay, was if lipid composition affects the membrane binding of EnB1. This question can be answered by looking at the overview of the fraction of bound protein in Figure 11 and at Table 4 below which specifies the lipid content of each sample.

Table 4. An overview of the sample components in lipid mixes 1, 2, 3, 7, and 8. The green rectangles marks the mixes to be compared with respect to their differing cardiolipin and cholesterol content. The purple rectangle highlights the cholesterol presence in each mix. *"++"* means that the double lipid amount was added, compared to the other samples.

	Cardiolipin	Cholesterol	DOPS	DOPE	DOPC	PI
Mix 1	+	+	+	+	-	-
Mix 2	-	+	+	+	-	-
Mix 3	+	-	+	+	-	-
Mix 7	++	-	-	+	+	+
Mix 8	+	-	-	+	+	+

To study how different lipids affect the membrane binding of EnB1, liposomes with CL and cholesterol can for instance be compared. The green and purple rectangles mark the CL and cholesterol mixes that are of interest to study when studying the difference in fraction of bound protein.

By looking at Figure 11 and Table 4 above, it is noticeable that the presence of CL is important for an improved EnB1 membrane binding. For instance, there is a significant difference of the binding capacity between Mix 1 and Mix 2, where Mix 1 contains CL and Mix 2 doesn't. This also coincides with the results of Mix 7 and Mix 8, where the double amount of CL enables more protein binding.

It can also be observed that CL in combination with cholesterol enables the most effective EnB1 binding in this experiment, see Mix 1 in Figure 11. This suggests that cholesterol also play an important role in protein-membrane binding, especially in combination with cardiolipin. However, Figure 11 demonstrates that CL without cholesterol allows for more protein binding, and not vice versa by comparing Mix 1 and 2. This indicates that CL is more important than cholesterol for protein-membrane binding.

The results in Figure 11 and Table 4 shows that lipid composition affects EnB1 membrane binding, both positively when CL and cholesterol are present, and negatively when other lipids are involved (see Table 5) below.

Table 5. An overview of the sample components in lipid mixes 4, 5 and 6. The blue rectangle highlights the presence of PIP_2 in each mix. *"++"* means that the double lipid amount was added, compared to the other samples.

	DOPE	DOPC	PI	PIP2
Mix 4	+	+	+	+
Mix 5	+	+	+	++
Mix 6	+	+	-	-

By comparing Mix 4, 5 and 6 by looking at Table 5 and Figure 11, it can be observed that the phosphoinositides PI and PIP_2 does not have a positive effect on the EnB1 binding. Mix 6, without PI and PIP_2, has the largest fraction of bound EnB1of these three mixes. It can also be observed that a double amount of PIP_2 in Mix 5 results in more protein binding compared to Mix 4.

These results demonstrates that these phosphoinositides does not appear to be important for this type of protein-membrane binding, as well as suggesting that a larger amount of PIP_2 enables more protein binding.

From the results of the fraction of bound protein displayed in Figure 11, it is shown that PIP_2 is not important for the recruitment of EnB1 to the membrane. All mixes containing PIP_2 showed a smaller fraction of bound protein relative to the other mixes without this specific lipid.

3.3.2 Curvature affects EnB1 membrane binding

The other main questions to be answer with this lipid binding assay, is how the curvature affect EnB1 binding. This question can be answered by looking at Figure 12 which shows the compiled result from Figure 11.

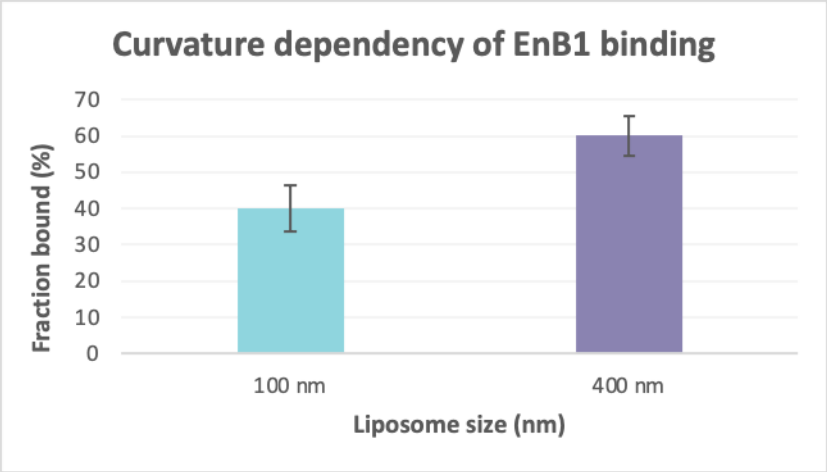

Figure 12. Bar graph displaying the difference between the bound fraction of EnB1 to the SUVs of 100 nm and LUVs of 400 nm for all lipid mixes in this project. The y-axis displays the fraction of bound EnB1 and the x-axis display the different liposome sizes. The data represents the mean ± SEM.

Figure 11 shows that most of the lipid mixes had more protein bound with larger liposomes of 400 nm. Mix 1 is an exception, where there are significantly more EnB1 bound to the smaller liposomes and both liposome sizes enable the same binding for Mix 8.

From Figure 12, which displays the overall binding capacity for each liposome size for all eight mixes, it is shown that the 400 nm liposomes enable more EnB1 binding compared to the 100 nm liposomes.

From the overview in Figure 11 and the summary in Figure 12, it can be seen that the fraction of bound protein differs with size, which concludes that the membrane curvature affects the membrane binding of EnB1.

3.4 Cryo-EM visualization

Cryo-EM was used to visualize EnB1 bound to a membrane template.

3.4.1 EnB1 remodeling

To study how the EnB1 membrane remodeling, liposomes with added EnB1 were analyzed.

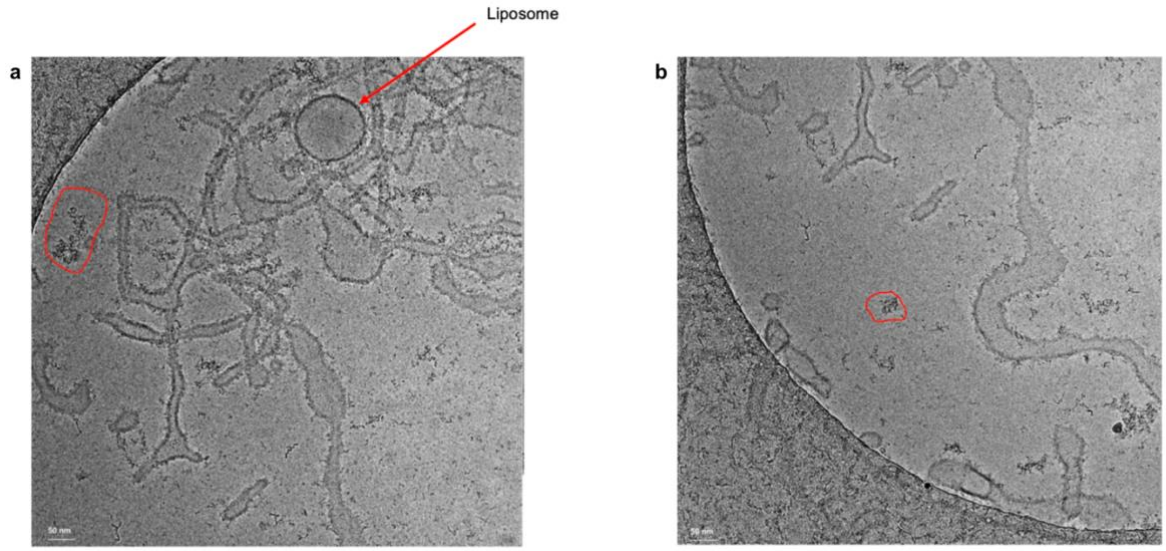

Figure 13. Cryo-EM visualization of EnB1 remodeling of 100 nm liposomes of Mix 1 with nominal magnification 92 000x. Scalebars of 50 nm is shown in the lower left corners. **a** EnB1 has caused liposome tubulation. Aggregated EnB1 is marked with a red circle. An intact liposome can also be observed. **b** EnB1 remodeling has resulted in liposome tubules of different sizes

Figure 13 confirms the abilities of EnB1 to remodel membranes. The tube-like structures of different sizes are tubulated liposomes. When tubulating a membrane, EnB1 forms a helical spiral and squeezes the liposome to a diameter of about 30 nm, which can be seen from the images in this figure.

4 Discussion

The aim of this project was to study how EnB1 interact with mimics of intracellular membranes. While interesting results have been obtained, new questions have also been raised. The first part of the discussion will focus on the main challenges with the nanodisc assembly. The results from the lipid binding assays showing that both the curvature and the lipid composition affects the EnB1 binding will also be discussed.

4.1 Nanodisc assembly

The nanodisc assembly was not thought to require as much optimization as it turned out be needed in the end. The most time-consuming step was to determine the optimal conditions for the detergent removal. A lot of time was consumed by trying to use the Bio Beads according to several protocols that had demonstrated successful results. For unknown reasons, the beads seemed to adsorb the lipids during the incubation. This could be confirmed since the lipids in were fluorescently stained and gave the whole sample a distinct color. After incubating the sample with the Bio Beads, it could clearly be seen that the beads had gained a pink color while the rest of the sample had become colorless, which indicates that there were no lipids or protein left in the sample. For further confirmation, the sample was purified with SEC which as expected did not detect any protein at all. The problem was attempted to be solved by incubation the beads with the sample in different temperatures and for different amounts of time, but the problem remained. Dialysis was therefore finally decided to be used instead. But since this step took longer than expected, there was no time to create more versions of nanodiscs as originally planned.

The only lipid mix used for the nanodisc assembly was DOPS. Since this lipid is negatively charged, the assembly process, as well as the binding capability of EnB1 to the lipid bilayer of the disc could be affected. Ideally, the optimal lipid mix determined by the liposome binding assay would have been used to create discs for the optimal EnB1 binding. In theory, this would have enabled more EnB1 binding to the discs, which would in turn beneficial for structural characterization with cryo-EM.

The optimized nanodiscs will be used be used by other members of the lab group for structural characterization of the bound EnB1 with cryo-EM.

4.2 Liposome binding assay

CL and cholesterol affect EnB1 binding

The lipid binding assay confirmed that CL is important for EnB1 binding and showed that cholesterol also appears to be important for EnB1 membrane binding, both in combination with CL (see Mix 1) and alone (see Mix 2). The SUVs for Mix 2 containing cholesterol, but no CL show a better result compared to the SUVs for Mix 3 that contain CL and no cholesterol. The LUVs on the other hand shows the opposite. This suggests that membranes with a high curvature of 100 nm and with a cholesterol content attracts more EnB1 to bind, compared to SUVs of the same size with CL. Membranes with a lower curvature and a CL content (see Mix 3, 7, 8) enables on the other hand more EnB1 binding compared to the LUVs with cholesterol.

The generally preferred binding to the liposomes with less curvature could be explained by the fact that the mitochondrial outer membrane also has a low curvature, which would explain why EnB1 would be more inclined to bind to this type of membrane. In theory, this would also motivate the higher fractions of bound protein to the membrane mimics containing CL, since CL is a mitochondria-specific phospholipid.

The combination of CL and cholesterol (Mix 1) gave the best result with almost 60% EnB1 binding to the 100 nm liposomes and approximately 50% EnB1 binding to the 400 nm liposomes. Interestingly, this was the only mix with SUVs that resulted in a higher percentage of bound protein compared to the LUVs. The other LUV mixes (Mix 2,3,7,8) containing either CL or cholesterol resulted in a lower fraction of bound EnB1.

The high fraction of bound protein for Mix 1 SUVs, could be explained by the fact that cholesterol normally is imbedded in the membrane and is in most cases not easily accessible for binding. The SUVs which cause a high curvature could however expose the imbedded cholesterol to the outside, since a higher curvature creates "gaps" in the outer membrane. These gaps could thereby enable EnB1 to sense the imbedded cholesterol and drive membrane binding.

In addition, it could also be suggested that there is some type of synergy between CL and cholesterol. This would also be interesting to investigate further. This could for instance be done by creating a mix with both cardiolipin and cholesterol, but with the double amount of cholesterol to see how the membrane binding would be affected. It would also be interesting to do more experiments where the amount of both lipids is gradually increased, to investigate which lipid ratio would be optimal for EnB1 binding.

PIP_2 does not seem to be important for the recruitment of EnB1 to the membrane

The results from Mix 4 and 5 which shows a low fraction of bound protein are not unexpected. As mentioned in the background, EnB1 doesn't have a positively charged amphipathic helix as EnA1 and is thereby not prone to bind to these kinds of liposomes. To investigate the actual difference in binding capacity of these two proteins, EnA1 could be added to liposomes of the exact same composition and size, and be used as a control.

Additionally, a larger amount of PIP_2 seems to enable more EnB1 binding. This could be due to the fact that this lipid contributes to more packing defects and positive membrane curvature which theoretically could attract more EnB1. Even though the double amount of PIP_2 contributes to more binding, the results show that EnB1 binds better to the liposomes without any PIP_2 present at all. As mentioned above, these results are not unexpected.

Nevertheless, none of these results involving Mix, 4, 5 and 6 are statistically significant, as shown in Table 3. This means that no final conclusions can be drawn from these results, since $p > 0.05$ for all these samples. The same experiments should therefore be repeated with larger sample sets to see if this will result in significant differences between the fractions of bound EnB1.

Membrane curvature is important for EnB1 binding

When studying how the membrane curvature affects EnB1 membrane binding, the results clearly show that a binding to LUVs with less curved membranes is favored compared to SUVs with more curvature. As mentioned above, this can be due to the fact that the mitochondria have an outer membrane with a relatively low curvature. Since EnB1 naturally binds to the MOM, this would explain why this protein is more inclined to bind to a membrane with a resembling curvature.

5 Conclusion & future prospects

The conclusions that can be drawn from the results in this project is that lipid composition and membrane curvature affect EnB1 binding. Is can also be concluded that CL is an important lipid for the binding of this protein. Further studies with larger sample sets and different mixes are however needed draw any final conclusions. Nevertheless, these results could be used as starting points for setting up more directed and detailed experiments to elucidate exactly how the EnB1-membrane binding mechanisms works. These findings could in the future be of interest in the field of cancer research, amongst many other related research fields.

6 Acknowledgments

I would like to thank my supervisor Anna Sundborger-Lunna for the opportunity to work on this interesting project, and for the time and efforts in guiding me. I would also like to thank Árni Thorlacius for all the help and supervision the lab. I also want to thank Tobias Hedström for the collaboration in the lab as well as all the fun discussions and laughs. Thanks to everyone in the ASL group and at the Structural Biology program for making me feel welcome from the start. I have had a great time doing this project and I have learnt a lot. I would also like to thank my subject reviewer Sebastian Barg for taking the time to review my project and for the valuable feedback and interesting discussions. Finally, I also want to thank my opponent Tanya Al-khafaf for your thoughts and comments on my report.

References

Balla T. 2013. Phosphoinositides: Tiny Lipids With Giant Impact on Cell Regulation. Physiological Reviews 93: 1019–1137.

Bayburt TH, Sligar SG. 2010. Membrane protein assembly into Nanodiscs. FEBS Letters 584: 1721–1727.

Bhatt VS, Ashley R, Sundborger-Lunna A. 2021. Amphipathic Motifs Regulate N-BAR Protein Endophilin B1 Auto-inhibition and Drive Membrane Remodeling. Structure 29: 61-69.e3.

Borges-Araújo L, Fernandes F. 2020. Structure and Lateral Organization of Phosphatidylinositol 4,5-bisphosphate. Molecules 25: 3885.

Chang-Ileto B, Frere SG, Chan RB, Voronov SV, Roux A, Di Paolo G. 2011. Synaptojanin 1-mediated PI(4,5)P2 hydrolysis is modulated by membrane curvature and facilitates membrane fission. Developmental cell 20: 206–218.

De Carlo S, Harris JR. 2011. Negative staining and cryo-negative staining of macromolecules and viruses for TEM. Micron 42: 117–131.

Denisov IG, Sligar SG. 2016. Nanodiscs for structural and functional studies of membrane proteins. Nature Structural & Molecular Biology 23: 481–486.

Doerr A. 2016. Single-particle cryo-electron microscopy. Nature Methods 13: 23–23.
Dudek J. 2017. Role of Cardiolipin in Mitochondrial Signaling Pathways. Frontiers in Cell and Developmental Biology 5:

Elías-Wolff F, Lindén M, P. Lyubartsev A, G. Brandt E. 2019. Curvature sensing by cardiolipin in simulated buckled membranes. Soft Matter 15: 792–802.

Emami S, Azadmard-Damirchi S, Peighambardoust SH, Valizadeh H, Hesari J. 2016. Liposomes as carrier vehicles for functional compounds in food sector. Journal of Experimental Nanoscience 11: 737–759.

Etxebarria A, Terrones O, Yamaguchi H, Landajuela A, Landeta O, Antonsson B, Wang H-G, Basañez G. 2009. Endophilin B1/Bif-1 Stimulates BAX Activation Independently from Its Capacity to Produce Large Scale Membrane Morphological Rearrangements*. The Journal of Biological Chemistry 284: 4200–4212.

Falabella M, Vernon HJ, Hanna MG, Claypool SM, Pitceathly RDS. 2021. Cardiolipin, Mitochondria, and Neurological Disease. Trends in Endocrinology & Metabolism 32: 224–237.

Goldie KN, Abeyrathne P, Kebbel F, Chami M, Ringler P, Stahlberg H. 2014. Cryo-electron Microscopy of Membrane Proteins. In: Kuo J (ed.). Electron Microscopy: Methods and Protocols, pp. 325–341. Humana Press, Totowa, NJ.

Karbowski M, Jeong S-Y, Youle RJ. 2004. Endophilin B1 is required for the maintenance of mitochondrial morphology. The Journal of Cell Biology 166: 1027–1039.
Kühlbrandt W. 2015. Structure and function of mitochondrial membrane protein complexes. BMC Biology 13: 89.

Lacapère J-J, Pebay-Peyroula E, Neumann J-M, Etchebest C. 2007. Determining membrane protein structures: still a challenge! Trends in Biochemical Sciences 32: 259–270.

Lipa-Castro A, Legrand F-X, Barratt G. 2021. Cochleate drug delivery systems: An approach to their characterization. International Journal of Pharmaceutics 610: 121225.

Lyumkis D. 2019. Challenges and opportunities in cryo-EM single-particle analysis. The Journal of Biological Chemistry 294: 5181–5197.

Masuda M, Takeda S, Sone M, Ohki T, Mori H, Kamioka Y, Mochizuki N. 2006. Endophilin BAR domain drives membrane curvature by two newly identified structure-based mechanisms. The EMBO Journal 25: 2889–2897.

Nakhaei P, Margiana R, Bokov DO, Abdelbasset WK, Jadidi Kouhbanani MA, Varma RS, Marofi F, Jarahian M, Beheshtkhoo N. 2021. Liposomes: Structure, Biomedical Applications, and Stability Parameters With Emphasis on Cholesterol. Frontiers in Bioengineering and Biotechnology 9:

Paila YD, Chattopadhyay A. 2010. Membrane Cholesterol in the Function and Organization of G-Protein Coupled Receptors. In: Harris JR (ed.). Cholesterol Binding and Cholesterol Transport Proteins: Structure and Function in Health and Disease, pp. 439–466. Springer Netherlands, Dordrecht.

Ramadurai S, Holt A, Krasnikov V, van den Bogaart G, Killian JA, Poolman B. 2009. Lateral Diffusion of Membrane Proteins. Journal of the American Chemical Society 131: 12650–12656.

Salzer U, Kostan J, Djinović-Carugo K. 2017. Deciphering the BAR code of membrane modulators. Cellular and Molecular Life Sciences 74: 2413–2438.

Sarkis J, Vié V. 2020. Biomimetic Models to Investigate Membrane Biophysics Affecting Lipid–Protein Interaction. Frontiers in Bioengineering and Biotechnology 8:

Shukla S, Jin R, Robustelli J, Zimmerman ZE, Baumgart T. 2019. PIP2 Reshapes Membranes through Asymmetric Desorption. Biophysical Journal 117: 962–974.

Simunovic M, Voth GA, Callan-Jones A, Bassereau P. 2015. When Physics Takes Over: BAR Proteins and Membrane Curvature. Trends in Cell Biology 25: 780–792.

Wang W, Yang L, Huang HW. 2007. Evidence of Cholesterol Accumulated in High Curvature Regions: Implication to the Curvature Elastic Energy for Lipid Mixtures. Biophysical Journal 92: 2819–2830.

Zheng H, Handing KB, Zimmerman MD, Shabalin IG, Almo SC, Minor W. 2015. X-ray crystallography over the past decade for novel drug discovery – where are we heading next? Expert opinion on drug discovery 10: 975–989.

Zhukovsky MA, Filograna A, Luini A, Corda D, Valente C. 2019. Phosphatidic acid in membrane rearrangements. FEBS Letters 593: 2428–2451.

7 Appendix

7.1 Lipid mixes

MIX 1

Lipid	%	Conc. (mg/ml)	Vol. (uL)
DOPS	50	10	25
DOPE	40	10	20
Cardiolipin	5	0.1	250
Cholesterol	5	20	1.25

MIX 2

Lipid	%	Conc. (mg/ml)	Vol. (uL)
DOPS	55	10	27.5
DOPE	40	10	20
Cholesterol	5	20	1.25

MIX 3

Lipid	%	Conc. (mg/ml)	Vol. (uL)
DOPS	55	10	27.5
DOPE	40	10	20
Cardiolipin	5	0.1	250

MIX 4

Lipid	%	Conc. (mg/ml)	Vol. (uL)
DOPC	37	10	18.5
DOPE	44	10	22
PIP_2	10	10	5
PI	9	20	4.5

MIX 5

Lipid	%	Conc. (mg/ml)	Vol. (uL)
DOPC	33	10	16.5
DOPE	38	10	19
PI	9	10	4.5
PIP_2	20	10	10

MIX 6

Lipid	%	Conc. (mg/ml)	Vol. (uL)
DOPC	50	10	25
DOPE	50	10	25

MIX 7

Lipid	%	Conc. (mg/ml)	Vol. (uL)
DOPC	33	10	16.5
DOPE	38	10	19
PI	9	10	4.5
Cardiolipin	20	10	10

MIX 8

Lipid	%	Conc. (mg/ml)	Vol. (uL)
DOPC	46	10	23
DOPE	38	10	19
PI	9	10	4.5
Cardiolipin	7	10	3.5

7.2 Statistical analysis

```
#Master Thesis project
#Sigrid Mack, 2022-05-14
#ANOVA & Post Hoc & t-test for liposome binding assay

Mix1.100 <- c();#add values for mix 1
Mix2.100 <- c(); #add values for mix 2
Mix3.100 <- c(); #add values for mix 3



#combines the data into a singe data set
Combined_Groups <- data.frame(cbind(Mix1.100, Mix2.100, Mix3.100));
Combined_Groups; #shows result
summary(Combined_Groups); #min, median, mean, max

Stacked_Groups <- stack(Combined_Groups);
Stacked_Groups; #shows table

#ANOVA-test
Anova_Results <- aov(values ~ ind, data = Stacked_Groups);
summary(Anova_Results); #shows ANOVA result


#Posthoc Test
Posthoc <- TukeyHSD(Anova_Results);
show(Posthoc)

#t-test; 2-tailed distribution; assume equal variance
ttest <-t.test(Mix1.100, Mix2.100);
show(ttest)
```